



Title	Tunneling anisotropic magnetoresistance in epitaxial CoFe/n-GaAs junctions
Author(s)	Uemura, Tetsuya; Imai, Yosuke; Harada, Masanobu; Matsuda, Ken-ichi; Yamamoto, Masafumi
Citation	Applied Physics Letters, 94(18), 182502 https://doi.org/10.1063/1.3130092
Issue Date	2009-05-04
Doc URL	http://hdl.handle.net/2115/38547
Rights	Copyright 2009 American Institute of Physics. This article may be downloaded for personal use only. Any other use requires prior permission of the author and the American Institute of Physics. The following article appeared in ,Appl. Phys. Lett. 94, 182502 (2009), and may be found at https://dx.doi.org/10.1063/1.3130092
Type	article
File Information	94-18_182502.pdf



[Instructions for use](#)

Tunneling anisotropic magnetoresistance in epitaxial CoFe/*n*-GaAs junctions

Tetsuya Uemura,^{a)} Yosuke Imai, Masanobu Harada, Ken-ichi Matsuda, and Masafumi Yamamoto

Division of Electronics for Informatics, Hokkaido University, Sapporo 060-0814, Japan

(Received 25 March 2009; accepted 14 April 2009; published online 4 May 2009)

Magnetic and transport properties of a fully epitaxial CoFe/*n*-GaAs junction were investigated. The CoFe film grown on the GaAs showed strong magnetic anisotropy in which uniaxial anisotropy with an easy axis of $[1\bar{1}0]$ dominated with a slight cubic anisotropy having easy axes of $[110]$ and $[1\bar{1}0]$ superimposed. Tunneling anisotropic magnetoresistance (TAMR) was observed at 4.2 K in the CoFe/*n*-GaAs junction. Angular dependence of the tunnel resistance showed uniaxial-type anisotropic tunnel resistance between the $[110]$ and $[1\bar{1}0]$ directions in the (001) plane that varied strongly with a bias voltage. The observed TAMR effect can be explained by the anisotropic electronic structure due to Rashba and Dresselhaus spin-orbit interactions. © 2009 American Institute of Physics. [DOI: 10.1063/1.3130092]

A spin-valve-like magnetoresistance (MR), referred to as tunneling anisotropic MR (TAMR), was recently found in (Ga, Mn)As-based magnetic tunnel junctions (MTJs)^{1,2} and CoFe/MgO/CoFe MTJs.³ Unlike the tunneling MR effect, in which the tunnel resistance changes depending on the relative orientation of the magnetizations (whether parallel or antiparallel) of the two independent ferromagnetic electrodes in the MTJs, the TAMR effect produces a change in the tunnel resistance for MTJs with the parallel magnetization configuration depending on the absolute direction of the magnetizations with respect to the crystal axes. The TAMR is attributed to the anisotropic density of states for tunneling electrons due to spin-orbit interactions (SOIs).¹ Furthermore, there have been several reports on the TAMR effect in junctions with a single ferromagnetic electrode, such as (Ga, Mn)As/ AlO_x /Au,⁴ Fe/*i*-GaAs/Au,⁵ (Co/Pt)_{*n*}/ AlO_x /Pt,⁶ and CoFeB/MgO/*n*-GaAs.⁷ Since the TAMR can produce a spin-valve-like effect with only a single ferromagnetic electrode, it is essential to investigate the TAMR effect in junctions having a single ferromagnetic electrode rather than in the MTJ structures.

Interestingly, the TAMR effect occurs also in ferromagnet/semiconductor junctions as reported in Ref. 5. This suggests that the TAMR effect would affect the properties of spin injection devices using ferromagnet/semiconductor heterostructures, particularly spin transistors,^{8,9} in which a MR effect between the ferromagnetic source and drain electrodes caused by spin polarized electrons injected from the source plays an important role in the device operation. The structure given in Ref. 5, in which a thin undoped GaAs layer acting as a tunnel barrier is sandwiched between Fe and Au electrodes, differs from those of typical spin injection devices. Thus, it is important to investigate the TAMR effect in more straightforward structures for the clarification of the influence of the TAMR effect on spin injection devices. In this study, we prepared an epitaxial CoFe thin film on *n*-GaAs, whose structure is similar to the channel structure of a typical spin injection device¹⁰ and in-

vestigated the TAMR effect of the CoFe/*n*-GaAs junctions. We also investigated magnetic properties of the CoFe thin film grown on the *n*-GaAs and discuss the possible origin of both the magnetocrystalline anisotropy and the TAMR.

Layer structures consisting of (from the substrate side) *i*-GaAs (50 nm)/*n*⁻-GaAs (Si = $1 \times 10^{16} \text{ cm}^{-3}$, 750 nm)/*n*⁺-GaAs (Si = $3 \times 10^{18} \text{ cm}^{-3}$, 30 nm) were grown by molecular beam epitaxy at 580 °C on GaAs(001) substrates. This channel structure was similar to that described in Ref. 10, where electrical spin injection and detection using a Fe electrode were reported. The *n*⁺-GaAs layer was inserted to reduce the Schottky barrier width, resulting in the tunnel conduction becoming dominant. The sample was then capped with an arsenic protective layer and transported to an ultrahigh-vacuum magnetron-sputtering chamber with a base pressure of about 6×10^{-8} Pa. Prior to the growth, the arsenic cap was removed by heating the sample to 400 °C. A 20-nm-thick Co₅₀Fe₅₀ (CoFe) film and a 5-nm-thick Ru capping layer were grown by magnetron sputtering at room temperature (RT).

X-ray pole figure measurement confirmed that a CoFe film was epitaxially grown on the GaAs with a cube-on-cube relation. Figure 1 shows the magnetic hysteresis curves of an epitaxial CoFe film measured at RT. A magnetic field (*H*) was applied along the $[110]$ and $[1\bar{1}0]$ directions. Saturation magnetization of approximately 1700 emu/cm³ was obtained, a value comparable to that typically reported in the bulk sample. The CoFe film showed strong magnetic anisotropy. In addition to cubic anisotropy imposed by the crystal symmetry of CoFe with easy axes of $[110]$ and $[1\bar{1}0]$, uniaxial anisotropy with an easy axis in the $[1\bar{1}0]$ direction was observed because of structural and/or electronic asymmetry of the CoFe/GaAs interface between $[110]$ and $[1\bar{1}0]$, as discussed later.

Next we will describe the transport properties of CoFe/*n*-GaAs junctions. Figure 2 shows MR curves at 4.2 K with measuring circuits for (a) a lateral CoFe/*n*-GaAs/CoFe junction consisting of two CoFe/*n*-GaAs junctions and (b) a CoFe/*n*-GaAs single junction. The size of each junction mea-

^{a)}Electronic mail: uemura@ist.hokudai.ac.jp.

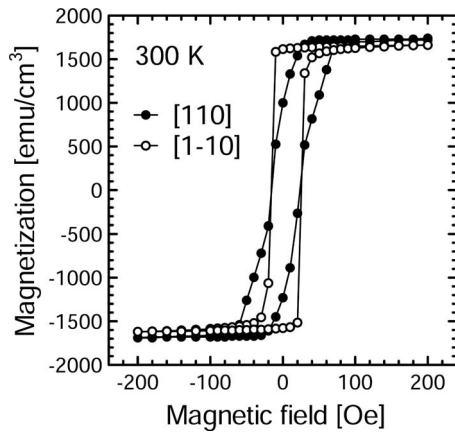


FIG. 1. Magnetization as a function of applied field (H) for an epitaxial $\text{Co}_{50}\text{Fe}_{50}$ film grown on an n -GaAs measured at RT. H was applied along the $[110]$ and $[1\bar{1}0]$ directions.

sured in Fig. 2(a) were 10×50 and $15 \times 50 \mu\text{m}^2$, and the spacing between them was $2 \mu\text{m}$, while the size of the junction measured in Fig. 2(b) was $10 \times 50 \mu\text{m}^2$. A constant current of 10 nA was supplied to each junction and H was applied along the $[110]$ direction. The circuit configuration shown in Fig. 2(a) measures the resistance between two CoFe electrodes through the n -GaAs, including the series resistance of two CoFe/ n -GaAs junctions, while the circuit configuration shown in Fig. 2(b) measures the resistance between the CoFe and the n -GaAs in the middle junction. A clear MR change was observed for both cases. Since the MR value shown in Fig. 2(a) was almost equal to the sum of the MR value of each junction, the origin for the MR change was the same in both cases. We will hereafter consider the MR characteristics of the CoFe/ n -GaAs single junction shown in Fig. 2(b). Since H was applied along the $[110]$ direction, low resistance states at sufficiently high magnetic fields of $|H| > 200$ Oe correspond to states in which the magnetization (M) of the CoFe lies along the $[110]$ or $[\bar{1}\bar{1}0]$ direction. On the other hand, high resistance states at small

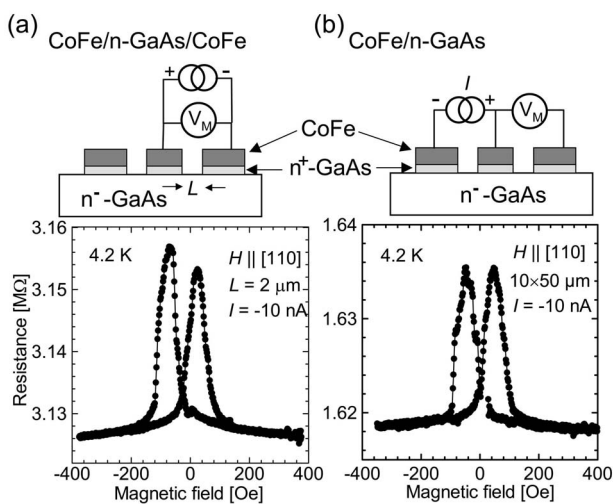


FIG. 2. MR characteristics at 4.2 K for (a) a lateral CoFe/ n -GaAs/CoFe junction, and (b) a CoFe/ n -GaAs junction. The circuit configurations are also shown. The size of each junction measured in (a) were 10×50 and $15 \times 50 \mu\text{m}^2$, and the spacing between them was $2 \mu\text{m}$. The size of the junction measured in (b) was $10 \times 50 \mu\text{m}^2$. The magnetic field was applied along the $[110]$ direction. The bias current was 10 nA.

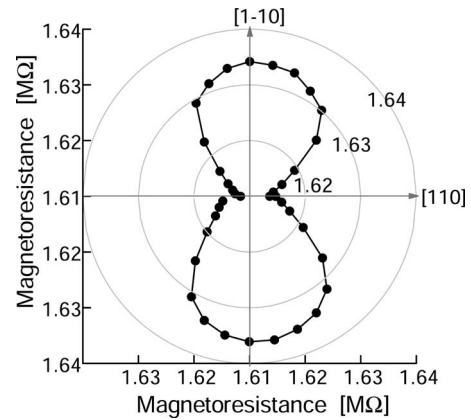


FIG. 3. Polar plot of tunnel magnetoresistance at 4.2 K under $H = 1000$ Oe in the CoFe/ n -GaAs junction. The polar angle is defined with respect to the $[110]$ direction.

magnetic fields of $|H| < 200$ Oe correspond to states in which M is oriented to other directions during a magnetization reversal. Therefore, it is most probable that the peak of the MR curve is due to the state in which M of the CoFe lies along the $[1\bar{1}0]$ or $[\bar{1}10]$ direction.

To confirm the relation described above between the resistance value and the magnetization direction of CoFe, we investigated the dependence of the MR value on the direction of M . Figure 3 shows a polar plot of the MR value at 4.2 K under $H = 1000$ Oe, where M was forced to align along the direction of H by applying a sufficiently high magnetic field. The polar angle in the figure indicates the angle between the direction of M and the $[110]$ direction. The figure clearly shows a uniaxial-type anisotropic MR value with respect to in-plane M . The MR value took a maximum at $\theta = \pm 90^\circ$ ($M \parallel [1\bar{1}0]$ or $M \parallel [\bar{1}10]$) and a minimum at $\theta = 0$ or 180° ($M \parallel [110]$ or $M \parallel [\bar{1}\bar{1}0]$), with an MR ratio of approximately 1.3%. The observed MR change cannot be explained by either an anisotropic MR (AMR) effect of the CoFe electrode (estimated to be less than about 10Ω) and that caused by the local Hall effect (estimated to be less than 1Ω) were much smaller than the observed MR change (about $20 \text{ k}\Omega$), indicating that the TAMR was dominant in the MR change. Note that since the TAMR effect induces the MR change at each junction, it affects the MR characteristics of a device consisting of a lateral ferromagnet/semiconductor-channel/ferromagnet structure, as shown in Fig. 2(a).

The bias voltage (V) dependence of the MR ratio clearly showed that the MR ratio decreased as the magnitude of V increased for both polarities. Here, we defined the MR ratio by $r = (R_{1\bar{1}0} - R_{110}) / R_{110}$, where R_{110} and $R_{1\bar{1}0}$ stand for MR values at $M \parallel [110]$ and $[1\bar{1}0]$, respectively. The bias voltage was defined with respect to the n -GaAs. Interestingly, a negative MR ratio was obtained at $V \geq 0.2$ V. Figure 4 shows MR curves with different forward bias voltages close to 0.2 V. R_{110} was smaller than $R_{1\bar{1}0}$ when $V < 0.2$ V (positive MR ratio) but larger when $V \geq 0.2$ V (negative MR ratio). Such switching between the positive and negative MR ratios depending on the bias voltage was also reported for the Fe/ i -GaAs/Au vertical junction of Ref. 5.

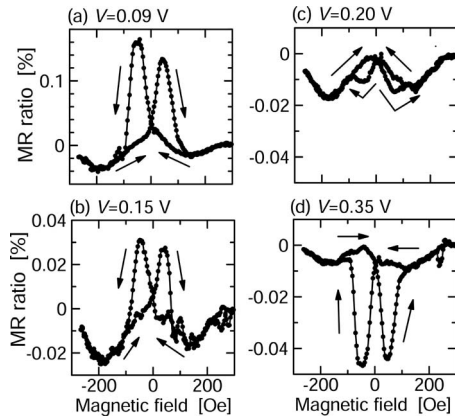


FIG. 4. MR curves at 4.2 K with different bias voltages of (a) +0.09 V, (b) +0.15 V, (c) +0.20 V, and (d) +0.35 V. The bias voltage was defined with respect to the *n*-GaAs.

We observed uniaxial-type anisotropy between the $[110]$ and $[1\bar{1}0]$ directions for both the crystalline magnetoanisotropy and the tunnel resistance in the epitaxial CoFe/*n*-GaAs junction. We will discuss the origin of these anisotropic natures. Uniaxial-type magnetic anisotropy similar to that shown in Fig. 1 has been reported in several previous studies,^{11–18} in particular for Fe (Ref. 11) or Co-based Heusler alloy thin films^{12–18} grown on GaAs. There have been several theoretical models for the symmetry of the GaAs substrate, such as a surface reconstruction of GaAs, formation of an interface alloy, or anisotropic interfacial bonds.¹⁶ Although these models based on the structural asymmetry of the GaAs substrate might be able to explain the nonequivalent tunnel resistance between R_{110} and $R_{1\bar{1}0}$, they cannot explain the results for the bias voltage dependence of the MR, in particular the switching behavior between the positive and negative MR ratios depending on the bias voltage, as shown in Fig. 4.

A possible theoretical model based on the combination of Rashba and Dresselhaus SOIs was proposed for the origin of the TAMR, including its bias voltage dependence.⁵ We will briefly summarize the consequences of Rashba and Dresselhaus terms on the electronic structure in the CoFe/*n*-GaAs. The Hamiltonian for the SOIs is given by

$$\hat{H}_{\text{SO}} = \alpha(\sigma_x k_y - \sigma_y k_x) + \beta(\sigma_x k_x - \sigma_y k_y), \quad (1)$$

where α and β are the effective Rashba and Dresselhaus parameters, σ_x and σ_y are Pauli spin matrices, and k_x and k_y are the electron wave vectors. Here, the *x*-axis and *y*-axis are set to the $[100]$ and $[010]$ directions, and only electrons with $k_z \approx 0$ are considered. The eigenvalues of the total Hamiltonian are given by

$$E = \begin{cases} \varepsilon(\vec{k}) \pm (\alpha - \beta)|\vec{k}| & (\vec{k} \parallel [1\bar{1}0]), \\ \varepsilon(\vec{k}) \pm (\alpha + \beta)|\vec{k}| & (\vec{k} \parallel [110]), \end{cases} \quad (2)$$

where $\varepsilon(\vec{k})$ is the electron energy without the SOI. Equation (2) indicates that the $[110]$ and $[1\bar{1}0]$ axes become non-equivalent in the presence of both Rashba and Dresselhaus SOIs, consequently producing the TAMR. According to this model, one can explain the switching behavior between the positive and negative MR ratios in terms of the sign of $\alpha\beta$. For example, if $\alpha\beta > 0$, then the second term of Eq. (2) for

$[1\bar{1}0]$ becomes smaller than that for $[110]$, and vice versa. If the sign of α and/or β as well as their magnitude are assumed to be voltage dependent, one can explain the bias voltage dependence of the MR ratio. The SOI-based model, therefore, explains more reasonably the TAMR effect than those based on the structural asymmetry of the CoFe/GaAs interface. For a (Ga,Mn)As system, correlation between the magnetoanisotropy and the TAMR was reported,² both of which originated from strong SOIs in the valence band of (Ga, Mn)As. As for the CoFe/GaAs system, however, it is still unclear whether the SOI-based model can explain also the uniaxial-type magnetic anisotropy. To fully understand the correlation between the TAMR and the magnetoanisotropy, further systematic studies are necessary.

In conclusion, we observed uniaxial-type TAMR between the $[110]$ and $[1\bar{1}0]$ directions in the epitaxial CoFe/*n*-GaAs junction. The observed TAMR effect that varied strongly with the bias voltage can be explained by the anisotropic electronic structure due to Rashba and Dresselhaus SOIs. We found that the TAMR effect possibly affects the device operation of spintronic devices consisting of ferromagnet/semiconductor heterostructures, e.g., spin injection devices.

This work was supported in part by a Grant-in-Aid for Scientific Research (A) (Grant No. 20246054), a Grant-in-Aid for Scientific Research on Priority Area “Creation and control of spin current” (Grant No. 19048001), and a Grant-in-Aid for Scientific Research (C) (Grant No. 19560307), from the MEXT, Japan.

¹C. Rüster, C. Gould, T. Jungwirth, J. Sinova, G. M. Schott, R. Giraud, K. Brunner, G. Schmidt, and L. W. Molenkamp, *Phys. Rev. Lett.* **94**, 027203 (2005).

²H. Saito, S. Yuasa, and K. Ando, *Phys. Rev. Lett.* **95**, 086604 (2005).

³L. Gao, X. Jiang, S. Yang, J. D. Burton, E. Y. Tsymal, and S. S. P. Parkin, *Phys. Rev. Lett.* **99**, 226602 (2007).

⁴C. Gould, C. Rüster, T. Jungwirth, E. Girgis, G. M. Schott, R. Giraud, K. Brunner, G. Schmidt, and L. W. Molenkamp, *Phys. Rev. Lett.* **93**, 117203 (2004).

⁵J. Moser, A. Matos-Abiague, D. Schuh, W. Wegscheider, J. Fabian, and D. Weiss, *Phys. Rev. Lett.* **99**, 056601 (2007).

⁶B. G. Park, J. Wunderlich, D. A. Williams, S. J. Joo, K. Y. Jung, K. H. Shin, K. Olejnik, A. B. Shick, and T. Jungwirth, *Phys. Rev. Lett.* **100**, 087204 (2008).

⁷T. Inokuchi, T. Marukame, M. Ishikawa, H. Sugiyama, and Y. Saito, *Appl. Phys. Express* **2**, 023006 (2009).

⁸S. Datta and B. Das, *Appl. Phys. Lett.* **56**, 665 (1990).

⁹S. Sugahara and M. Tanaka, *Appl. Phys. Lett.* **84**, 2307 (2004).

¹⁰X. Lou, C. Adelman, S. A. Crooker, E. S. Garlid, J. Zhang, K. S. M. Reddy, S. D. Flexner, C. J. Palmström, and P. A. Crowell, *Nat. Phys.* **3**, 197 (2007).

¹¹J. M. Florczak and E. D. Dahlberg, *Phys. Rev. B* **44**, 9338 (1991).

¹²T. Ambrose, J. J. Krebs, and G. A. Prinz, *Appl. Phys. Lett.* **76**, 3280 (2000).

¹³A. Hirohata, H. Kurebayashi, S. Okamura, N. Tezuka, and K. Inomata, *IEEE Trans. Magn.* **41**, 2802 (2005).

¹⁴T. Uemura, T. Yano, K.-I. Matsuda, and M. Yamamoto, *Thin Solid Films* **515**, 8013 (2007).

¹⁵T. Yano, T. Uemura, K.-i. Matsuda, and M. Yamamoto, *J. Appl. Phys.* **101**, 063904 (2007).

¹⁶W. H. Wang, M. Przybylski, W. Kuch, L. I. Chelaru, J. Wang, Y. F. Lu, J. Barthel, H. L. Meyerheim, and J. Kirschner, *Phys. Rev. B* **71**, 144416 (2005).

¹⁷T. Uemura, Y. Imai, S. Kawagishi, K.-I. Matsuda, and M. Yamamoto, *Physica E* **40**, 2025 (2008).

¹⁸S. Kawagishi, T. Uemura, Y. Imai, K.-i. Matsuda, and M. Yamamoto, *J. Appl. Phys.* **103**, 07A703 (2008).